THE JOURNAL OF PHYSICAL CHEMISTRY B

Article

pubs.acs.org/JPCB

NMR Investigation of Chloromethane Complexes of Cryptophane-A and Its Analogue with Butoxy Groups

Z. Takacs,[†] E. Steiner,[†] J. Kowalewski,*[,†] and T. Brotin[‡]

[†]Department of Materials and Environmental Chemistry, Arrhenius Laboratory Stockholm University, SE-106 91 Stockholm, Sweden

[‡]Laboratoire de Chimie (CNRS-UMR 5182), École Normale Supérieure de Lyon, 46 Allée d'Italie, F-69364 Lyon Cedex 07, France

Supporting Information

ABSTRACT: Host–guest complexes between cryptophane-A as host and dichloromethane and chloroform as guests are investigated using ^{1}H and ^{13}C NMR spectroscopy. Moreover, a related cryptophane, with the methoxy groups replaced by butoxy units (cryptophane-But), and its complexes with the same guests were also studied. Variable temperature spectra showed effects of chemical exchange between the free and bound guests, as well as of conformational exchange of the host. The guest exchange was studied quantitatively by exchange spectroscopy or line shape analysis. Extraction of kinetic and thermodynamic parameters led to the characterization of the affinity between guests and hosts. On the other hand, the host exchange was investigated by means of ^{13}C Carr–Purcell–Meiboom–Gill (CPMG) relaxation dispersion which aims at the determination of the transverse relaxation rate R_2, the inverse of the transverse relaxation time T_2, as a function of the repetition of the π pulses in a CPMG train. The variation of the measured transverse relaxation rate with the repetition rate ν_{CPMG} indicated conformational exchange occurring on the microsecond–millisecond time scale. Structural information was obtained through measurements of cross-relaxation rates, both within the host and between the host and the guest protons. The NMR results were supported by DFT calculations.

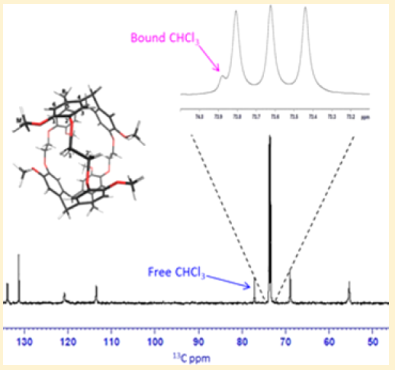

INTRODUCTION

Cryptophane-A was the first cryptophane synthesized by Collet et al. in 1981.[1,2] It is composed of two equivalent cyclotribenzylene (CTB) caps bound together by three ethylenedioxy linkers. On each phenyl ring, there is one methoxy group. Cryptophane-A has been the subject of many interesting studies in the field of host–guest chemistry. It has a hydrophobic three-dimensional cavity capable of binding small organic molecules such as chloromethanes[3,4] as well as xenon atoms.[5] The investigation of these molecular entities helps to understand molecular recognition. The previously investigated chloromethane complexes of cryptophane-C revealed a surprisingly high affinity constant for dichloromethane and relatively low affinity constant for chloroform.[6] This has brought up the question of what structural properties have the largest effect on the complexation. Cryptophane-A and -C are both *anti*-isomers, but the latter has nonequivalent caps with only one of the caps carrying the methoxy substituents on the phenyl groups (see molecules 1 and 2 in Scheme 1).

Apart from this, the two molecules 1 and 2 are identical. They also have the same cavity volumes. As will be discussed in the present work, cryptophane-A in solution is in exchange between its conformers similarly to cryptophane-C. The encapsulation of a chloromethane guest changes the probability distribution of the conformers as it has been seen before.[6,7] Nuclear magnetic resonance (NMR) is a perfect tool for characterizing the encapsulation process but also for following the guest-induced changes in the host. These chemical events can be explained, for instance, by means of NMR spin–echo experiments. In this work, translational diffusion was investigated in order to reveal the eventual presence of another guest, water, inside the host cavity.[8] Carr–Purcell–Meiboom–Gill (CPMG) relaxation dispersion methodology[9,10] was dedicated to shed light on the host conformational exchange. Obviously, upon encapsulation, both ^{1}H and ^{13}C spectra displayed changes of the peak positions. It is not only the peak position that is very informative but also the intensity and broadening of the guest ^{1}H signal in the free and bound position, in particular if the host and the guest are present in close to the 1:1 molar ratio. This concentration ratio also allows a better estimation of the affinity constant from the ^{1}H spectrum. The comparison of the data to cryptophane-C is not

Scheme 1. Structures of Cryptophane-A (Molecule 1), Cryptophane-C (Molecule 2), and Cryptophane-But (Molecule 3)

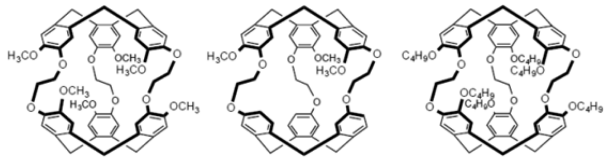

Received: October 24, 2013
Revised: January 28, 2014
Published: January 28, 2014

   dx.doi.org/10.1021/jp4105272 | J. Phys. Chem. B 2014, 118, 2134–2146

sufficient to draw the final conclusion concerning the relation between the structure of the caps and the affinity. To complete the analysis, another cryptophane-A derivative was chosen in which the methoxy groups attached to the CTB rings were replaced by butoxy groups, resulting in a third cryptophane with the same cavity volume (see molecule 3 in Scheme 1). The *trans*-conformers of cryptophane-A are shown in Figure 1, and its analogue with butoxy groups replacing the methoxy substituents, denoted cryptophane-But, is shown in Figure 2.

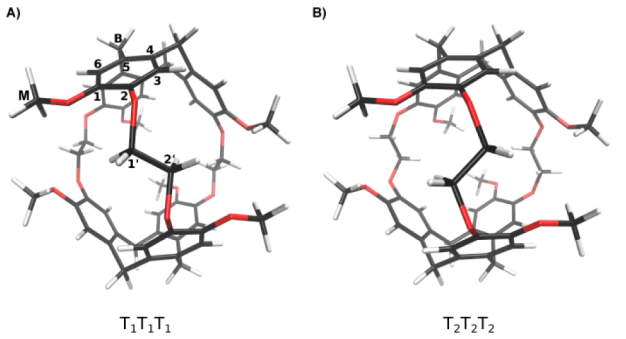

Figure 1. (A) The $T_1T_1T_1$ conformer of cryptophane-A with the atom numbering. (B) The $T_2T_2T_2$ conformer of cryptophane-A.

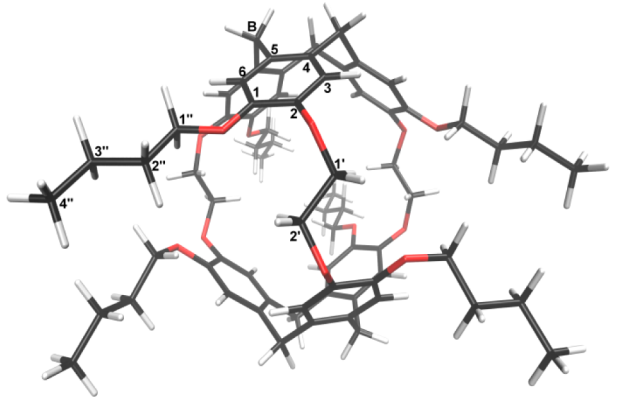

Figure 2. The $T_2T_2T_2$ conformer of cryptophane-But.

EXPERIMENTAL SECTION

Sample Preparations. Cryptophane-A and cryptophane-But were synthesized by Brotin et al.[11,12] ^{13}C labeled chloroform and the deuterated solvent, 1,1,2,2-tetrachloroethane-d_2, were obtained from Cambridge Isotope Laboratory. Nonlabeled chloroform was obtained from Sigma Aldrich and dichloromethane from Scharlau Chemie S.A. The commercially obtained chemicals were used without further purification.

The raw solid cryptophanes contained $CHCl_3$, CH_2Cl_2, and ethanol coming from the recrystallization. A 30 mM solution of cryptophane-A was prepared without any purification (sample 1). Another solution, sample 2, with 10 mM cryptophane-A containing 60 mM added nonlabeled chloroform was prepared with no purification. For quantitative analysis, the material was dipped into nonlabeled chloroform or dichloromethane and the solvent was then let to evaporate. The process was repeated three times. For quantitative work, the following solutions in 1,1,2,2-tetrachloroethane-d_2 were prepared:

(3) 12 mM cryptophane-A and 13 mM CH_2Cl_2
(4) 11 mM cryptophane-But and 13 mM CH_2Cl_2
(5) 10 mM cryptophane-A and 11 mM $CHCl_3$
(6) 11 mM cryptophane-But and 12 mM $CHCl_3$
(7) 20 mM cryptophane-A and 15 mM CH_2Cl_2
(8) 10 mM cryptophane-A and 62 mM $^{13}CHCl_3$
(9) 10 mM cryptophane-But and 90 mM $^{13}CHCl_3$
(10) 10 mM cryptophane-But and 25 mM $CHCl_3$
(11) 10 mM cryptophane-But, 9 mM $CHCl_3$, and 6.5 mM CH_2Cl_2
(12) 30 mM cryptophane-A and 150 mM $CHCl_3$

The solubility of cryptophane-A in tetrachloroethane is much higher than that of cryptophane-C and cryptophane-But.

NMR Spectroscopy. ^1H and ^{13}C experiments were performed with Bruker Avance spectrometers operating at 9.4, 14.1, and 16.5 T using 5 mm (BBI and BBO at 9.4 T, TXI and BBO at 14.1 T, and cryo-TXI at 16.5 T) probe heads. At 9.4 T, the temperature calibration was done using a standard methanol calibration sample, while a resistance detector made of copper wire dipped into silicon oil contained in a 5 mm NMR tube was used at the two higher fields. The accuracy of the temperature determination is estimated at ±1 K. All the experiments measuring build-up or decay were repeated at least twice. The peak assignment was based on DQF-COSY, (2D) NOESY, (2D) ROESY, as well as $^1H-^{13}C$ edited HSQC experiments.

The EXSY measurements were performed at 250 K and 16.5 T using the implementation as the DPFGSENOE sequence with two selectively refocusing shaped pulses and one hard π pulse in the middle of the mixing time interval.[13] The semi-selective inversion pulses were implemented as Gaussian G3 cascades[14] with a duration of 18−20 ms. Sixteen different time intervals were used. Experiments were performed with 64 accumulated signal transients, using a relaxation delay of 35−40 s. Only the doublets of the ^{13}C-labeled chloroform were evaluated. The purpose of the label is to enhance the proton spin−lattice relaxation. The evaluation of the exchange rate of the forward (complexation) reaction was based on the approach proposed originally by Macura et al.[15] and described by Hu and Krishnamurthy.[16] The exchange rate of the backward (decomplexation) reaction was based on the principle of detailed balance, in order to avoid the error coming from small intensities at very short mixing times in the initial rate regime.[7]

^{13}C spectra were recorded with Waltz16 proton decoupling at 9.4 T, while Waltz65 was used at 14.1 and 16.5 T. The decoupling power corresponded, on average, to the nutation frequency of 2.8 kHz. The spin−lattice relaxation times of the guest ($^{13}CHCl_3$) were measured by the inversion−recovery method using 16−19 recovery delays ranging from 0.5 ms to 30 s with a relaxation delay of 35 s. The heteronuclear Overhauser enhancement was measured with the dynamic NOE sequence.[17] The NOE build-up period was set to $5T_1$ and the relaxation delay to $10T_1$. In the spectrum with no NOE enhancement, the build-up period was set to 0.1 ms.

The 2D NOESY and ROESY at 9.4 and 14.1 T were recorded at 235, 240, 255, and 258 K. The detection method used was States -TPPI. The mixing times were 0.02−0.24 s for the NOESY and 0.04−0.2 s for the ROESY. The spin lock power was set to 3 kHz. In the direct dimension, 8 scans were used with 16 dummy scans, with a relaxation delay of 5−7 s. The size of the direct FID was 4096 data points, giving an approximately 0.6 s acquisition time in the t_2 domain. 512 and 768 data points were used in the indirect (t_1) dimension, which were zero filed to 4096 points. The window functions in both dimensions were shifted quadratic sine bell functions. The NOESY pulse sequence contained a hard

dx.doi.org/10.1021/jp4105272 | J. Phys. Chem. B 2014, 118, 2134−2146

π-pulse in the middle of the mixing time and two z gradients with a power of 40% and −40% of the maximum value.[18] The ROESY sequence used was $\pi/2$-t_1-spin lock-t_2.[19,20] The volume integrals were used for data analysis. The ROESY spectra were only used for qualitative analysis.

The ^{1}H diffusion experiments were performed at 258 and 268 K using a pulse-gradient stimulated echo (PGSTE) sequence with a longitudinal eddy-current delay (LED) and bipolar gradient pulses. Two spoil gradients were also applied during the longitudinal storage periods.[21] The calibration of the gradients was accomplished by measuring the diffusion coefficient of a well-known sample at 298 K.[22] In our case, the Bruker standard "doped water" sample which is composed of 1% H_2O in D_2O with 0.1 g/L $GdCl_3$ was used. During the diffusion experiments, the gradient strength was linearly incremented in 32 steps from 2 to 95% of its maximum value; the diffusion time Δ and the gradient pulse duration δ were kept constant.

The ^{13}C CPMG measurements were performed at two static magnetic fields (B_0 = 14.1 and 16.5 T) and two temperatures (T = 298 and 310 K). The carbons 1′ and 2′ corresponding to the cryptophane-A linkers and the aromatic carbon 6 (see Figure 1) were considered. The transverse relaxation rates R_2 were measured using a ^{13}C Carr−Purcell−Meiboom−Gill (CPMG) sequence with proton decoupling during acquisition and a proton 180° pulse at every second echo in the ^{13}C CPMG pulse train to avoid the CSA-DD cross-correlation effects.[23] For each R_2 measurement, the delay between the 180° pulses in the CPMG pulse train, ν_{CPMG}, was kept constant while the number of 180° pulses was increased. Every experiment was recorded with 1024 scans and 16 dummy scans with a relaxation delay of 2 s. The ^{13}C CPMG relaxation dispersions were established for ν_{CPMG} (=$1/(2\tau_{CPMG})$) values ranging from 166.7 to 2500 Hz.

Quantum Chemical Calculations. All calculations were performed in a similar way as reported for cryptophane D and C.[6,7] The Gaussian 09 package[24] was used. Geometries were optimized at the level of the DFT-B3LYP functional with the basis set 6-31G(d). Each optimized structure was then taken and a single point energy calculation was done, together with the calculation of the ^{13}C chemical shift using the GIAO method,[25] with the larger basis set 6-311+G(2d,p). The calculated chemical shifts reported are referenced to the calculated chemical shift of TMS at the same level of theory. All the calculations were performed using the conductor polarizable continuum model (CPCM)[26,27] with the parameters appropriate for dichloroethane solvent. Two sets of calculations were made: one for the empty host and one with a chloroform molecule inside the cavity. The van der Waals interaction was taken into consideration in all structures optimized with the B3LYP functional by adding, after the geometry optimization, the empirical term to the DFT energies.[28]

RESULTS

Guest-Related Kinetics and Thermodynamics. Following our earlier work,[7] the complex formation in the host−guest (H−G) systems is described in terms of the reaction

$$H + G \underset{k_{-1}}{\overset{k_1}{\rightleftarrows}} HG \tag{1}$$

NMR methods allow investigation of the reaction kinetics at equilibrium, when the concentrations of various species are constant in time. The forward and backward processes are individually described by the rate expressions:

$$-\frac{d[G]}{dt} = k_1[H][G] = k_1'[G] \tag{2}$$

$$-\frac{d[HG]}{dt} = k_{-1}[HG] \tag{3}$$

The (pseudo) first-order rate constants, k_{fb} (free-to-bound) and k_{bf} (bound-to-free), are defined according to

$$k_{fb} = k_1' = k_1[H] \quad \text{and} \quad k_{bf} = k_{-1} \tag{4}$$

The equilibrium constant for the complex formation (the affinity constant) is given by

$$K = \frac{[HG]}{[H][G]} = \frac{k_1}{k_{-1}} = \frac{k_{fb}}{[H]k_{bf}} \tag{5}$$

Equation 5 can be reformulated in terms of the principle of detailed balance:

$$k_{fb}[G] = k_{bf}[HG] \tag{6}$$

Equations 1−6 form the basis of the discussion of the kinetics and thermodynamics of our systems.

Cryptophane-A. The solutions with approximately 1:1 host:guest ratios (samples 3−6) are very informative compared to the solutions with high guest excess (samples 8−10 and 12). In the case of samples 3−6, the intensity and the integral of the bound guest peak are higher than those for the free guest. This implies a relatively high affinity to the host. In order to extract more information on kinetics, namely, the exchange rates, it is possible to perform line-shape fitting[29,30] on the spectra in which the exchange caused line-broadening is higher than $1/T_2$*, i.e., the combined effect of the natural line width in the absence of exchange and magnetic field inhomogeneity. This is not a problem in the case of the dichloromethane guest, since, even at the lowest temperature (235 K), the exchange-caused line-broadening is large (see Figure 3). The results of the line-shape fitting are summarized in Table 1.

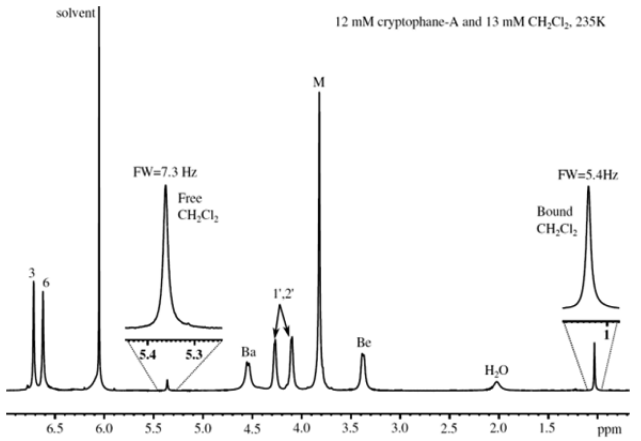

Figure 3. The proton spectrum of CH_2Cl_2@cryptophane-A in 1,1,2,2-$C_2D_2Cl_4$ (sample 3) at 14.1 T and 235 K.

In the case of $CHCl_3$@cryptophane-A at low temperatures, the exchange of the guest is not fast enough for line-shape fitting. The rate constants k_{fb} reported in Table 1 at 235, 245, and 255 K were obtained from the EXSY experiments,[7] while k_{bf} were calculated from the principle of detailed balance. The populations were calculated from the integrals in the spectrum. The rates and

dx.doi.org/10.1021/jp4105272 | J. Phys. Chem. B 2014, 118, 2134−2146

Table 1. Population of the Bound Site p_b and Kinetic Data for Dichloromethane and Chloroform Complexes of Cryptophane-A[a]

host:	cryptophane-A									
guest:	CH_2Cl_2					$CHCl_3$				
T (K)	p_b	k_{fb} (s^{-1})	k_{bf} (s^{-1})	k_1 (s^{-1} M^{-1})	K (M^{-1})	p_b	k_{fb} (s^{-1})	k_{bf} (s^{-1})	k_1 (s^{-1} M^{-1})	K (M^{-1})
235	0.78	17	5	8600	1800	0.76	**0.3**	**0.01**	190	2000
245	0.77	48	14	24200	1700	0.75	**1.3**	**0.5**	720	1600
255	0.76	110	34	53200	1600	0.73	**5.2**	**1.9**	2600	1300
265	0.75	267	87	121300	1400	0.71	18.7	7.7	8500	1100
275	0.74	732	253	312900	1200	0.66	38	20	14100	730
285	0.68	1366	658	423600	640	0.62	72	45	22500	510
305						0.50	167	168	37100	220

[a]The exchange rates in the case of $CHCl_3$ at 235, 245, and 255 K (bold font) were determined by EXSY experiments, in other cases by line-shape fitting (samples 3 and 5). The equilibrium constant (K) was calculated from the concentrations of the species.

populations for $CHCl_3$@cryptophane-A at higher temperatures are based on the line-shape fitting.[29,30]

The exchange of dichloromethane is faster than that of chloroform. This can be explained by the size difference between the two guests (indeed, the van der Waals volumes of dichloromethane and chloroform are, respectively, equal to 55 and 72 Å^3).[31] For both guests, the exchange is much slower than in the case of cryptophane-C. The only difference between the two hosts is that cryptophane-C has nonequivalent caps, since the methoxy groups are missing from one of them. A hypothesis formulated in our recent cryptophane-C study[6] is that the methoxy groups block the entrance and exit of the cavity. In the case of cryptophane-A, the methoxy groups from the caps (see Figure 1) present an even more severe hindrance for the guest. Thus, the corresponding exchange processes are expected to be slower for cryptophane-A, in agreement with the present observations.

In the case of both guests, the ratio $k_{fb}/k_{bf} = [HG]/[G]$ is very high. This means that the affinity of cryptophane-A is very high both to chloroform and to dichloromethane. Knowing the total concentrations of the compounds, one can calculate the concentration of the species ([H], [G], [HG], see the Supporting Information) and calculate the equilibrium constant at every temperature. From Table 1, the affinity constant is higher for chloroform than for dichloromethane at 235 K. This is interesting, since chloroform is the bigger guest, which might be expected to fit worse inside the host cavity. It is also noteworthy that the equilibrium constant determined here for the dichloromethane guest is much higher than it was reported in earlier work from our laboratories,[4] where a large excess of dichloromethane compared to the cryptophanes led to a large uncertainty in the free host concentration.

Cryptophane-But. The data analysis of the solutions containing cryptophane-But and dichloromethane is difficult because the exchange at low temperatures is rather slow and only the integrals can be used for estimating the approximate concentration of the species present. An example of the ^{1}H spectrum of sample 4 at 245 K is shown in Figure 4.

Nevertheless, it is possible to calculate the populations of the free site p_f and of the bound site p_b (where $p_b = 1 - p_f$) at this temperature range (see Table 2). At higher temperatures, overlap occurs between the bound guest and the signals from the butoxy groups.

For $CHCl_3$@cryptophane-But, it was possible to measure signal integrals at the low temperatures (235 and 245 K) and to perform the line shape analysis between 255 and 305 K. Comparing the values of the bound site population p_b in Tables 1 and 2, one can notice that the bound site population is the highest out of the four complexes in the case of CH_2Cl_2@cryptophane-But.

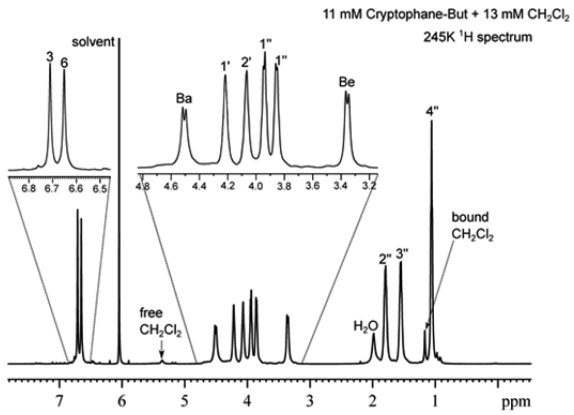

Figure 4. The proton spectrum of CH_2Cl_2@cryptophane-But in 1,1,2,2-$C_2D_2Cl_4$ (sample 4) at 14.1 T and 245 K.

The equilibrium constant values for both complexes are very high, falling actually in the range where NMR is not the most suitable technique. The values reported here for the dichloromethane complex carry a big error, since the concentration of the host is very low (see the Supporting Information) and the baseline and integration error sum up. Nevertheless, it is still possible to draw the conclusion that the equilibrium constant is very high. Surprisingly, the exchange is faster in the case of $CHCl_3$@cryptophane-But than $CHCl_3$@cryptophane-A, while the affinity constants are similar. A possible explanation of this observation (as suggested by one of the reviewers) is that the bulky butoxy groups cannot organize in the closed conformation (see below).

Activation Parameters. Summarizing the exchange rates between free and complexed sites, one can state that the $CHCl_3$ guest is typically in slow exchange, while CH_2Cl_2 exchanges faster on the chemical shift time scale. Using the Arrhenius and Van't Hoff equations, it is possible to estimate the activation energy and the reaction enthalpy of the complexation reactions (see the Supporting Information). The data for k_1 and $k_{-1} = k_{bf}$ are summarized in Table 3.

The activation energy obtained for the CH_2Cl_2@cryptophane-A system agrees with previous studies.[4] The activation energies for the $CHCl_3$@cryptophane-A are the highest, which agrees well with structure and size considerations such as the previously mentioned blocking effect of the methoxy groups connected to the CTB rings. The lower activation energy of $CHCl_3$@

dx.doi.org/10.1021/jp4105272 | J. Phys. Chem. B 2014, 118, 2134−2146

Table 2. Population of the Bound Site p_b and Kinetic Data for Dichloromethane and Chloroform Complexes of Cryptophane-But (Samples 4 and 6)

host:	cryptophane-But									
guest:	CH_2Cl_2					$CHCl_3$				
T (K)	p_b	k_{fb} (s^{-1})	k_{bf} (s^{-1})	k_1 (s^{-1} M^{-1})	K (M^{-1})	p_b	k_{fb} (s^{-1})	k_{bf} (s^{-1})	k_1 (s^{-1} M^{-1})	K (M^{-1})
235	0.82				15500	0.81	6.3	1.5	4800	3200
245	0.82				11000	0.80	8.6	2.2	6100	2900
255	0.79				5500	0.78	12.5	3.5	7800	2300
265						0.75	34.8	11.7	17400	1500
275						0.72	68.5	26.1	28500	1100
285						0.70	155	68	59600	900
305						0.61	387	245	105000	420

Table 3. Arrhenius Activation Energies and Reaction Enthalpies and Entropies for All the Investigated Systems

host:	cryptophane-A				cryptophane-But			
guest:	CH_2Cl_2		$CHCl_3$		CH_2Cl_2		$CHCl_3$	
reaction:	k_1	k_{-1}	k_1	k_{-1}	k_1	k_{-1}	k_1	k_{-1}
E_a (kJ·mol^{-1})	45	54	46	77			29	46
$E_a(k_{-1}) - E_a(k_1)$	9		31				17	
ΔH (kJ·mol^{-1})	−5		−20		−26		−18	
ΔS (J·mol^{-1}·K^{-1})	41		−13		−28		−6	

cryptophane-But indicates also that the butoxy groups play a role in the complexation dynamics, but it is not as obvious as in the case of cryptophane-A.

Looking at these results, it is worthwhile to not forget to take account of experimental errors coming from the sample preparation, the integration, and the line-shape fitting. The estimated error of total concentrations is 20% (based on repeated sample preparations) and is obviously propagated to the association constant K and the exchange rate constant k_1 (the other parameters, determined by integration or by line-shape fitting, carry a lower error which can be estimated around 5%) . The samples containing close to 1:1 molar ratio of the host and the guest also suffer from the low intensity of the peak of the free site. This is, on the other hand, the consequence of the high affinity constant which was "hidden" in earlier work by the high excess of the guest.

Chloroform Mobility Inside the Cavity (^{13}C T_1 and NOE). In order to probe the mobility of the guest within the cryptophane cavity, relaxation of chloroform, both in the free and the bound state, was investigated. The longitudinal relaxation rate R_1 (inverse of the longitudinal relaxation time T_1) and the heteronuclear NOE were measured for the ^{13}C of the guest, in analogy with earlier work from our laboratories.[4,6,7,32,33] The relaxation data obtained at 250 K are summarized in Table 4.

From this table, one can see that, when chloroform is free in the solution, extreme narrowing conditions are achieved; indeed, the ^{13}C spin-relaxation rate R_1 is independent of the magnetic field and a full NOE is retrieved. Concerning the bound chloroform, the reported values show a field dependence of the longitudinal relaxation rate R_1 as well as a NOE enhancement less than full. In order to explain these results, the motion of $CHCl_3$ encapsulated in the cryptophane-A host cavity was analyzed using the Lipari−Szabo model.[34] For the global correlation time, the value of 2.7 ns, estimated from the plot of τ_R versus the temperature established earlier, was used.[4] The resulting square of the generalized order parameter, S^2, is also shown in the table. It can be seen that the Lipari−Szabo order parameter for the guest within the cryptophane cavities agrees quite well with the corresponding quantities from the solid state.[4,35,36] The S^2 value found is high, indicating that the motion of the $CHCl_3$ molecule is restricted inside the host cavity.

Table 4. ^{13}C Relaxation Data for $CHCl_3$ in Sample 6 at 250 K[a]

field	14.1 T		16.5 T	
relaxation parameter	R_1 (s^{-1})	NOE	R_1 (s^{-1})	NOE
free site	0.190(0.004)	2.92(0.36)	0.190(0.003)	2.95(0.38)
bound site	2.47(0.03)	1.29(0.18)	2.16(0.03)	1.24(0.16)
S^2	0.7(0.2)			

[a]Uncertainties are given in parentheses.

More than One Guest: Diffusion Measurements. As there is no doubt concerning the encapsulation of dichloromethane or chloroform within cryptophane, one can wonder if other species present in our solutions can enter the host cavity. The question can especially arise for water (all the samples contain a small amount of water coming from the walls of the glass materials), as its molecular size is smaller than the one of dichloromethane or chloroform. To bring out the possible encapsulation of water, ^1H diffusion experiments[8] were performed on sample 7 and were compared to the results obtained on a sample containing dichloromethane in the same solvent but without cryptophane. Self-diffusion coefficients for cryptophane-A, dichloromethane, and water are given in Table 5 for the two samples investigated and for the two temperatures considered (258 and 268 K).

First, one can observe that the diffusion coefficient of each species varies as expected with the temperature. The self-diffusion coefficient of CH_2Cl_2 in the sample containing the host (sample 7) is much lower than the one in the sample without cryptophane-A (roughly 4 times smaller at 258 K and 3 times smaller at 268 K), indicating changes in the translational motions

Table 5. Self-Diffusion Coefficients ($m^2 \cdot s^{-1}$) for Cryptophane-A ($D^{Cr\text{-}A}$), Dichloromethane ($D^{CH_2Cl_2}$), and Water (D^{H_2O})[a]

		258 K	268 K
sample without cryptophane-A	D^{H_2O}	$(9.7 \pm 0.3) \times 10^{-10}$	$(11.4 \pm 0.3) \times 10^{-10}$
	$D^{CH_2Cl_2}$	$(4.7 \pm 0.1) \times 10^{-10}$	$(5.3 \pm 0.1) \times 10^{-10}$
sample with cryptophane-A (sample 7)	D^{H_2O}	$(8.3 \pm 0.3) \times 10^{-10}$	$(10.8 \pm 0.3) \times 10^{-10}$
	$D^{CH_2Cl_2}$	$(1.2 \pm 0.1) \times 10^{-10}$	$(1.8 \pm 0.1) \times 10^{-10}$
	$D^{Cr\text{-}A}$	$(0.9 \pm 0.1) \times 10^{-10}$	$(1.0 \pm 0.1) \times 10^{-10}$

[a]Errors are deduced from Monte Carlo iterations.

dx.doi.org/10.1021/jp4105272 | J. Phys. Chem. B 2014, 118, 2134−2146

of CH_2Cl_2. Moreover, its diffusion coefficient at 258 K is close to the value found for cryptophane, which definitely proves that dichloromethane and cryptophane diffuse as one entity[37,38] at this temperature. At 268 K, $D^{CH_2Cl_2}$ is roughly 2 times larger than $D^{Cr\text{-}A}$. This larger diffusion coefficient can be explained by the fact that $D^{CH_2Cl_2}$ can be seen as an apparent diffusion coefficient to which the diffusion of both bound and free molecules contributes. Indeed, as the exchange is getting faster and the association constant decreases with the temperature, the contribution coming from the free dichloromethane is more important, leading $D^{CH_2Cl_2}$ to increase.

Looking now at the self-diffusion coefficients of water, D^{H_2O}, in the samples with and without cryptophane, it is interesting to notice that they do not evolve in the same way as for dichloromethane. Indeed, they are practically not affected by the presence of the cryptophane. Even if they slightly decrease, they are still 10 times larger than the diffusion coefficients of cryptophane. Consequently, water may be interacting with the cryptophane but does not enter the cavity in solution, thus proving the hydrophobicity of the host cavity.[39] This observation differs from the conclusions obtained in the solid state by Taratula et al.,[40] which were however obtained in the absence of other suitable guests.

Host Conformations in the Host–Guest Complexes. *^{1}H and ^{13}C Spectra.* In our earlier studies, it was shown that the complexation of chloromethane changes the probability distribution of the host conformers.[6,7] This has an effect on the chemical shifts in both the ^{1}H and ^{13}C spectra because they are the weighted averages of the chemical shifts of all the conformers in fast exchange in solution. The exchange between the host conformers is always fast in the investigated temperature range, as opposed to the guest exchange (discussed above) which can be both fast and slow in this range.

In the case of cryptophane-A and cryptophane-But, the equilibrium constant for both guests, chloroform and dichloromethane, is higher than in the case of previously investigated compounds. This means that, at low temperatures, when the equilibrium is shifted toward complex formation, even at low concentration of the guest (1:1 host:guest ratio) the complexed forms dominate the spectra. In order to investigate the influence of complexation on the conformational distribution, it is an advantage to look at spectra with low guest concentrations, at least lower than the total concentration of the host. One way to create these conditions is to work on samples containing more than one guest. For cryptophane-A, the ^{1}H and ^{13}C spectra of sample 1 (cryptophane-A containing solvents of purification) at 240 K are shown in Figures 5 and 6.

The solution contains not only the two chloromethanes but also ethanol. Nevertheless, one can see three sets of signals for the three complexed forms of the host. The chloroform complex is labeled with the capital latter A, the dichloromethane complex with B, and ethanol with C. Both spectra are very informative. At this temperature, the free peaks of the guest are too small to allow reliable integration or not even observable. The guests can be considered to be fully complexed. This is not a surprise for chloromethanes, knowing the high affinity of the host to these guests. Interestingly, the host also encapsulates ethanol coming from the purification of the material. It can be further seen in Figure 5 that the chloroform complex has only one peak for the linker protons (Figure 5, peak (A)1′,2′), in contrast to the other guests which have two peaks for the linker protons (Figure 5, peaks (B,C)1′,2′). This implies a more symmetric environment in the case of the chloroform complex. The two proton peaks in

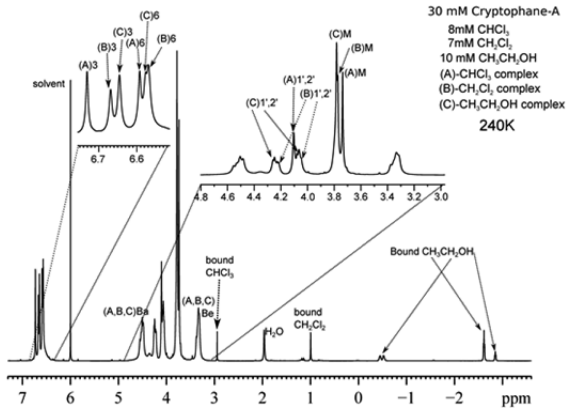

Figure 5. The ^{1}H spectrum of the solution containing 30 mM cryptophane-A, 8 mM $CHCl_3$, 7 mM CH_2Cl_2, and 10 mM CH_3CH_2OH in 1,1,2,2-$C_2D_2Cl_4$ (sample 1). The spectrum was recorded at 14.1 T and 240 K. The capital letter A denotes the $CHCl_3$@cryptophane-A, B the CH_2Cl_2 complex, and C the CH_3CH_2OH complex.

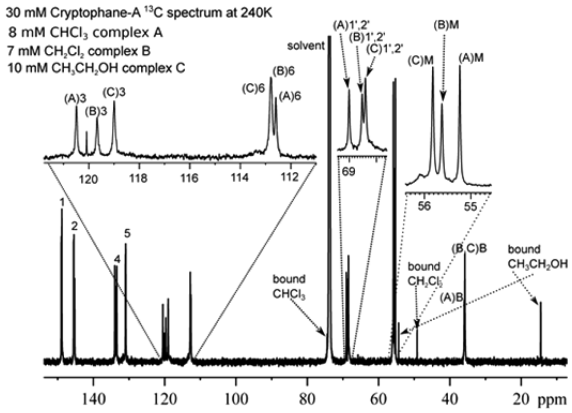

Figure 6. The ^{13}C spectrum of the solution containing 30 mM cryptophane-A, 8 mM $CHCl_3$, 7 mM CH_2Cl_2, and 10 mM CH_3CH_2OH in 1,1,2,2-$C_2D_2Cl_4$ (sample 1). The spectrum was recorded at 14.1 T and 240 K. The capital letter A denotes the $CHCl_3$@cryptophane-A, B the CH_2Cl_2 complex, and C the CH_3CH_2OH complex.

the case of other guests are dipolarly coupled to each other (cross-relaxed by each other), according to NOESY and ROESY spectra (see below). The aromatic region is also very informative. It can be seen that the difference between protons 3 and 6 is the biggest in the case of the chloroform complex and the smallest in the case of the ethanol complex.

In Figure 6, the ^{13}C spectrum of the same sample is shown. It is also possible to see here three separate sets of peaks for the three complexes (Figure 6, peak sets A, B, C). The spectrum shown here is a proton-decoupled ^{13}C spectrum which is easy to interpret; every peak represents a chemically and magnetically nonequivalent site in the molecule in question. One can make the following observations. The peak of the methoxy group is shifted upfield going from ethanol to chloroform guest (Figure 6, peaks (A)M, (B)M, and (C)M). The opposite behavior is true for the linker carbons. The signals belonging to the linkers are shifted downfield, and the chloroform complex has the highest chemical shift value. As in the case of the proton spectrum, the difference between the signals of the aromatic carbons is the highest in the case of the chloroform complex and the lowest in the case of the ethanol complex. If a high excess of chloroform (host:chloroform = 1:6, sample 2) is added to the same solution, it will "push" the

dx.doi.org/10.1021/jp4105272 | J. Phys. Chem. B 2014, 118, 2134–2146

other guests out of the cavity and the free guest peaks are observable again (see the Supporting Information). Figures 7 and 8 show the ^{1}H and ^{13}C spectrum of solution number 11 for the cryptophane-But complexes.

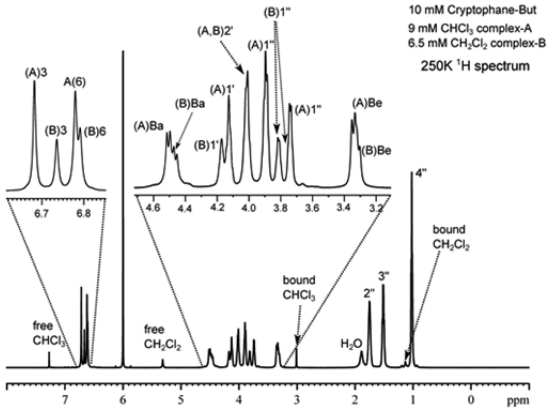

Figure 7. The ^{1}H spectrum of the solution containing 10 mM cryptophane-A, 9 mM $CHCl_3$, and 6.5 mM CH_2Cl_2 in 1,1,2,2-$C_2D_2Cl_4$ (sample 11). The spectrum was recorded at 16.5 T and 250 K. The capital letter A denotes the $CHCl_3$ and B the CH_2Cl_2 complex.

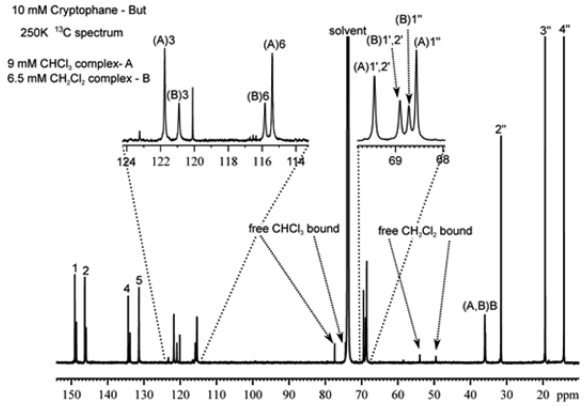

Figure 8. The ^{13}C spectrum of the solution containing 10 mM cryptophane-A, 9 mM $CHCl_3$, and 6.5 mM CH_2Cl_2 in 1,1,2,2-$C_2D_2Cl_4$ (sample 11). The spectrum was recorded at 16.5 T and 250 K. The capital letter A denotes the $CHCl_3$ and B the CH_2Cl_2 complex.

In this case, the sample does not contain any ethanol but only dichloromethane and chloroform in close to equimolar amount. Both spectra show exactly the same behavior concerning the chemical shift changes as in the previous case. By calculating the chemical shift differences of the aromatic carbon signals 3 and 6 ($\Delta = \delta_3 - \delta_6$), together with the full width at half-height (fwhh) of carbons 1′, 3, and 6 for the two hosts (see the Supporting Information), it can be seen that the signals at low temperatures are broadened by both conformational exchange of the hosts and the exchange of the guest. By increasing the temperature, both exchange processes are getting faster. The chemical shift difference of the aromatic carbons 3 and 6 is decreasing. This is due to the increasing amount of noncomplexed host, characterized by smaller Δ-values. At temperatures higher than 275 K, the peaks start to broaden again and, in the case of chloroform complexes, the peaks broaden into the baseline and further analysis is very difficult.

The spectra displayed in Figures 7 and 8 (sample 11) were recorded at 250 K. In the ^{1}H spectrum (Figure 7), it can be seen that the position of the bound CH_2Cl_2 peak is very close to signal number 4″ and other impurities, making, unfortunately, the integration difficult. Nevertheless, one can try to fit a Lorentzian to the peaks and extract information on the concentration ratio between bound and free CH_2Cl_2, because in this case not only the quantitative information is useful. The quantitative information can be used to get a better picture of the affinity of the host. The concentrations of various species are listed in Table 6.

Table 6. Concentration of Species in Solution 11 at 250 K

species/type	free (mM)	bound (mM)	bound/free
CH_2Cl_2	3.7	2.8	0.76
$CHCl_3$	3.6	5.4	1.50
host	1.8	8.2	4.56

One can see that the ratio $[HG]/[G] = k_{fb}/k_{bf}$ is much lower than that in Table 2. This is the effect of having two guests present at the same time. The data in Table 6 indicate that the affinities of cryptophane-But to both chloromethanes are rather similar.

Quantum Chemical Calculations of Chemical Shifts and Energies. The experimental information provided by the simple spectra is not sufficient to draw a definite conclusion on the type of conformers preferred by the different guests. In order to give a more detailed answer, one needs to look at the structure and symmetry properties of the conformers. In the case of cryptophane-A, the quantum chemical optimization was done previously by Brotin et al.[41] The present study complements that work by reporting also the chemical shifts of the ^{13}C sites in the conformers. Moreover, an attempt to correct the calculated energies with the van der Waals contribution[28] is performed here. As it was described in detail earlier,[6,7] the linkers can exist in various conformations. The all-*trans* conformers for cryptophane-A and cryptophane-But are shown in Figures 1 and 2, respectively. There are two types of *trans* conformers (both characterized by the -O-1′-2′-O- dihedral angle close to 180°) which differ in the relative orientation of the bond connecting carbons 1′ and 2′ with respect to the methoxy or butoxy groups on the CTB rings. The two orientations result in two very different conformers. Both $T_1T_1T_1$ and $T_2T_2T_2$ conformers belong to the D_3 point group. This means that there is no chemical shift difference between carbon number 1′ and 2′—these nuclei become symmetry-equivalent. A complication occurs when $CHCl_3$ enters the cavity: since it belongs to the C_{3v} symmetry group, it reduces the symmetry of the complex to C_3. The situation is different in the case of the *gauche* conformers. There are two basic types of *gauche* conformers, denoted G_+ and G_-, with the only difference in the sign of the -O-1′-2′-O- dihedral angle (+60°, −60°). Both all-*gauche* conformers belong to the C_3 symmetry group. This means that the equivalence of the linker carbons no longer holds: they have different chemical shifts. Additionally, there are also two types of G_+ and G_- conformers, which are denoted $G_{+,}$ G_{+b}, G_-, and G_{-b}. The difference between the conformers with and without subscript "b" is the orientation of the linker 1′−2′ bond with respect to the methoxy groups and, more importantly, to the other linkers. The three linkers can take different conformations independently of each other, which results in a large number of possible species. Two of the conformers are visualized in Figure 9.

The $G\_G\_G\_$ conformer is the molecule with black colored carbons, while the green molecule is the $G_{-b}G\_G\_$. Because of

dx.doi.org/10.1021/jp4105272 | J. Phys. Chem. B 2014, 118, 2134−2146

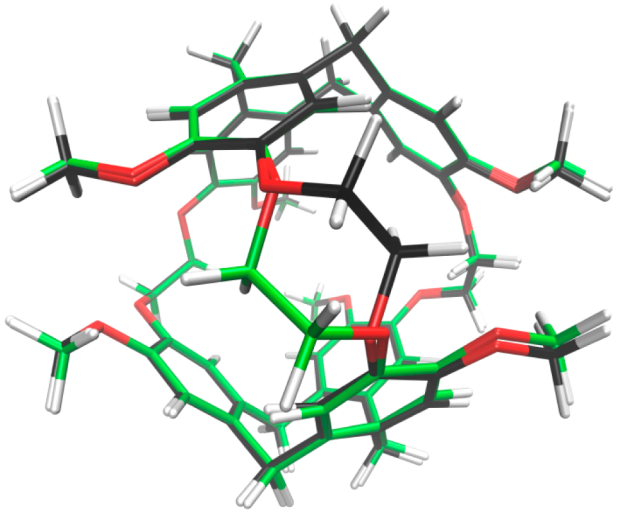

Figure 9. The $G\_G\_G\_$ and $G_{-b}G\_G\_$ conformers of cryptophane-A. The molecules are presented on top of each other. The molecule with black carbon framework is the $G\_G\_G\_$ conformer, and the green framework depicts the $G_{-b}G\_G\_$.

the equivalence of the caps, if one exchanges all the linkers from $G_{-,+}$ to $G_{-,+b}$, one gets back the original conformer; this means that the all-*gauche* conformers are pairwise equivalent (e.g., $G_{-b}G_{-b}G_{-b} = G\_G\_G\_$). The *gauche* conformers have one very important and useful property in common: the linker carbons are nonequivalent and their chemical shifts are different. The calculated chemical shifts are shown in Table 7.

As it can be seen in the table, when the *gauche* conformer changes to *gauche* b, the chemical shifts of the corresponding carbons 1′ and 2′ exchange places. This would not cause any complication, if the exchange of the linkers was synchronized, meaning that they only change simultaneously. This is not the case and the dynamics of the linkers can average the chemical shift to only one single peak, even if the symmetry of the conformers is only C_3. The picture is more complicated for protons. The chemical shifts and homonuclear *J*-couplings between the linker protons (there are four of them in each linker, with in principle different shifts and coupling, but they show up as two multiplets; see, e.g., Figure 5) are not averaged out for the dichloromethane (and ethanol) complex.

Table 7. Calculated Chemical Shifts (ppm) of the Linker Carbons When the Methoxy Groups Are Located in the Plane of Aromatics and Calculated Chemical Shifts (in ppm) of the Aromatic Carbons in $CHCl_3$@Cryptophane-A[a]

	conformer	1′	2′	$\Delta = \delta_{1'} - \delta_{2'}$
linker carbons (1′ and 2′)	$G_+G_+G_+$	71.8	73.9	−2.1
	$G_{+b}G_+G_+$	72.2	72.9	−0.7
	$G\_G\_G\_$	74.1	70.0	4.1
	$G_{-b}G\_G\_$	72.7	71.4	1.3
	$T_1T_1T_1$	75.0	75.0	0
	$T_2T_2T_2$	78.5	78.5	0
	conformer	3	6	$\Delta = \delta_3 - \delta_6$
aromatic carbons (3 and 6)	$T_1T_1T_1$A	129.1	116.8	12.3
	$T_1T_1T_1$B	129.7	131.1	−1.4
	$T_2T_2T_2$A	132.0	117.2	14.8
	$T_2T_2T_2$B	132.2	131.0	1.2
	$G_G_G_$A	123.1	116.5	6.7
	$G_G_G_$B	123.4	130.6	−7.2
	$G_+G_+G_+$A	122.0	117.1	4.9
	$G_+G_+G_+$B	124.0	121.8	2.2

[a]The capital letter A denotes a conformer optimized with a methoxy dihedral around zero. B denotes a conformer optimized with a methoxy dihedral of around −110°. The calculated shifts for the individual carbons differ by a few tenths of a ppm. Here, the average values are given.

The observed chemical shifts for the proton-carrying aromatic carbons also display conformation dependences. The situation of the chemical shifts of carbons 3 and 6 is more complicated, because of the close vicinity of the methoxy groups to number 6. The methoxy groups have two local minima. The one with lower energy corresponds to the methoxy groups in the plane of the aromatic rings, with the dihedral angle (6-1-O-M) around zero. When the same dihedral is around −110°, the methoxy group points out of the plane of the aromatic ring. The energy difference between these two methoxy group conformers is only about 6 kJ/mol, more or less independent of the linker conformation. The dynamic behavior of the methoxy groups plays an important role both in the kinetics of the complexation (as discussed in the case of cryptophane-C[6]) and in the chemical shift of the carbon number 6. The calculated chemical shifts and the difference between them are shown in Table 7.

There are two important conclusions that can be drawn looking at Table 7. The first is that the chemical shift difference between carbons 3 and 6 decreases going from the all-*trans* conformers to the all-*gauche* conformers. The second conclusion is that the orientation of the methoxy groups affects this difference dramatically. Namely, in the case of *trans* and *gauche*_ conformers, the order of the peaks (the sign of the Δ-value) is reversed. In the case of $gauche_+$, the Δ-value is reduced but still positive. From the HSQC and NOESY measurements, it is known that the order of the peaks 3 and 6 in the carbon spectrum is never exchanged. The explanation of this observation is that it almost never happens that all six of the methoxy groups are oriented with a dihedral angle of −110°. This, in turn, has an effect on the kinetics of the complex formation, since the reaction can only occur when two methoxy groups on the opposite sides of a "cavity window" point out of the aromatic plane. This is shown in Figure 10, where the conformer $G\_G\_G\_$ is displayed in the van der Waals representation when two methoxy groups on the opposite sides have a dihedral angle of zero (Figure 10A) and −110° (Figure 10B).

It can be seen that it is not possible for $CHCl_3$ to exit when the methoxy groups block the way. As anticipated above, this increased steric hindrance can be seen as the origin of the slower

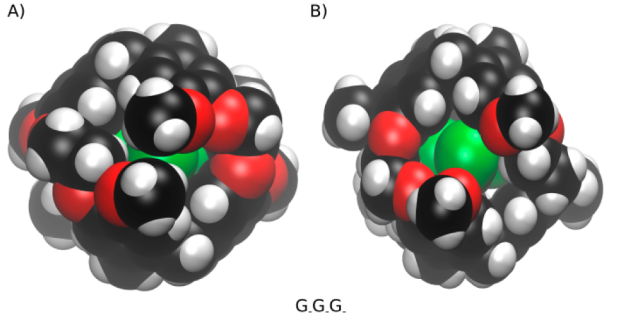

Figure 10. The van der Waals representation of the $G\_G\_G\_$ conformer of cryptophane-A. (A) The molecule with the 6-1-O-M dihedral angle close to zero, blocking the exit. (B) The molecule with the 6-1-O-M dihedral angle close to −110°, out of the way.

dx.doi.org/10.1021/jp4105272 | J. Phys. Chem. B 2014, 118, 2134−2146

dynamics of both guests@cryptophane-A compared to cryptophane-C.

Cryptophane-But is a larger molecule, and the DFT calculations are time-consuming. Due to this, the chemical shifts of only three noncomplexed ($G_+G_+G_+$, $T_1T_1T_1$, $T_2T_2T_2$) and two chloroform-complexed ($G_+G_+G_+$, $T_1T_1T_1$) conformers were calculated (see the Supporting Information). The results obtained are very similar to cryptophane-A. The shift difference between the proton-carrying aromatic carbons is highest in the case of the *trans* conformer and lowest in the case of the *gauche* conformer. The similarity also applies to the linker carbons. It is thus possible to summarize the findings as follows. The chemical shifts of the linker carbons are moved downfield (to higher shift values), if the *trans* character of the complex increases, and the shift difference, Δ, between the aromatic carbons also increases. However, with this information at hand, it is still not possible to decide which *trans* conformer is preferred by the complex. The only conclusion possible to draw is that the *trans* character increases in the case of binding of both chloromethane guests.

One possible help to decide which *trans* conformer is preferred by the complex can be provided by the DFT-calculated energies of the different complexes. The problem with the energies is that they are basis-set-dependent and that the contribution coming from the dispersion correction is an empirical estimate.[28] There are four types of energies one can compare. First, there are two energy values coming from the small and large basis set and containing only the zero point correction and the thermal contribution; in addition, there are the energies containing the dispersion contribution. From the relative energies of the noncomplexed cryptophane-A conformers with respect to the lowest values within the respective approximation level (see the Supporting Information), it can be seen that there are big differences between different calculations. In the case of no dispersion correction, the minimum occurs at the $T_1T_1T_1$ conformation with both basis sets and the dispersion-corrected energies have their minimum at the $G_{-b}G\_T_1$ conformer. This is a large difference. From the energy values, one can calculate the probability distribution of the conformers and weight the calculated chemical shifts with it. The weighted average of the shifts can be compared with the measured value. The calculated weighted average Δ-values for the small and large basis set are 11.6 and 10.6 ppm, respectively, which does not match with the measured values. Calculating the weighted chemical shifts in the same way, but using the dispersion-corrected energy data, one obtains 6.7 and 6.5 ppm. This is in better agreement with the experimental spectra. One has to keep in mind that in reality there was never any noncomplexed cryptophane-A in the solutions studied. The discussion thus refers to the dichloromethane and ethanol complex.

The situation is more complicated in the case of $CHCl_3$@cryptophane-A and $CHCl_3$@cryptophane-But complexes. First, as it was mentioned before, all the *gauche* conformers have at most C_3 symmetry. This also means that there is a difference in energy, dependent on the orientation of the chloroform molecule within the cavity. Figure 11 shows the $gauche_+$ conformer with the two orientations of chloroform.

It is also possible to change the linkers to $gauche_{+b}$ conformation and let the orientation of chloroform to remain unchanged. This complication arises only because the chloroform molecules cannot turn around in the cavity (see relaxation data above).

From the energies of the chloroform-complexed cryptophane-A (see the Supporting Information), it can be seen that, without

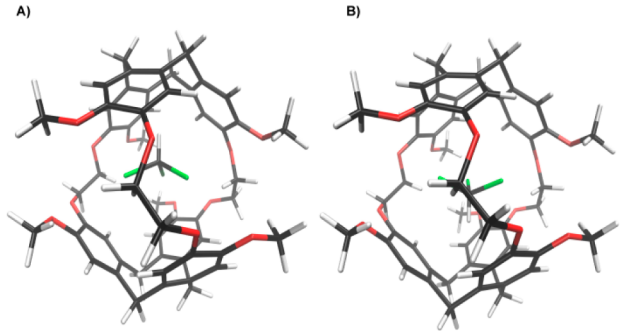

Figure 11. The two possible orientations of $CHCl_3$ inside the cavity of the $G\_G\_G\_$ conformer of cryptophane-A.

the dispersion correction, a minimum occurs at the $T_2T_2T_2$ with the small basis set and at the $G_{-b}T_1T_1$ conformer with the large basis set. For the dispersion-corrected data, the minimum is again changed drastically. This time, the minimum occurs at $G\_T_2T_2$ with the small basis set and at $G\_G\_G\_$ with the large basis set. Looking at the probability-weighted sum of the chemical shift differences between the proton-carrying aromatic carbons 3 and 6, one obtains similar values as before: 11.3 and 10.5 ppm without the dispersion correction and 10.5 and 8.6 ppm with the dispersion correction. It is thus confirmed again that the complexation of chloroform will increase this difference, but still it is not possible to select the preferred conformers.

^{13}C CPMG Relaxation Dispersion. So far, the only conclusion that can be drawn is that some guests prefer different conformations of the host. Thus, guests can either fit into major or minor states of the host. The main concern is that, due to a fast conformational exchange of the host (see above), minor states are not observable on the recorded spectra. Only a set of peaks corresponding to an average of these major and minor states is detectable. In order to get more information on this conformational or chemical exchange, the ^{13}C CPMG relaxation methodology,[9,10] which allows one to characterize physicochemical parameters of systems under conformational exchange, was applied on sample 12. As observed in Figures 12 and 13, the transverse relaxation rate R_2 of the linkers (singlet peak for carbons 1′ and 2′, as seen in Figure 6) and of the aromatic carbon

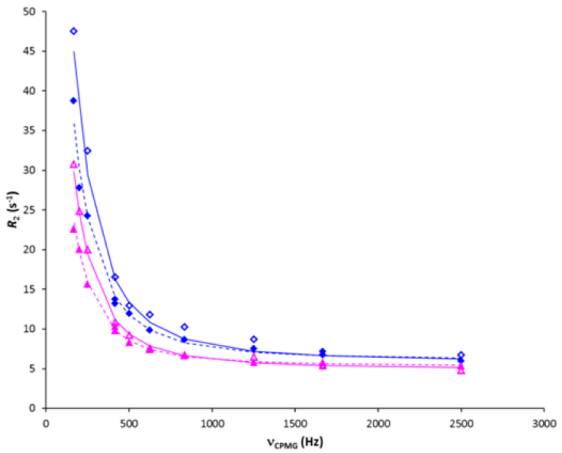

Figure 12. ^{13}C relaxation dispersion curves obtained for the cryptophane-A linkers (triangles) and the aromatic carbon 6 (lozenges) at 298 K (sample 12). Filled symbols, transverse relaxation rates R_2 obtained at 14.1 T; empty symbols, transverse relaxation rates R_2 obtained at 16.5 T.

dx.doi.org/10.1021/jp4105272 | J. Phys. Chem. B 2014, 118, 2134−2146

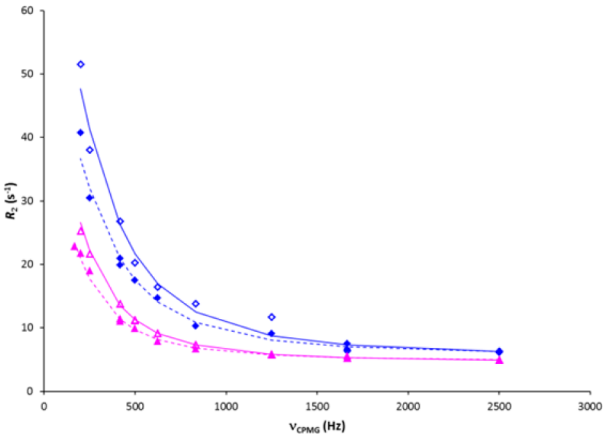

Figure 13. ^{13}C relaxation dispersion curves obtained for the cryptophane-A linkers (triangles) and the aromatic carbon 6 (lozenges) at 310 K (sample 12). Filled symbols, transverse relaxation rates R_2 obtained at 14.1 T; empty symbols, transverse relaxation rates R_2 obtained at 16.5 T.

6 varies as expected with the repetition rate ν_{CPMG} (=1/($2\tau_{CPMG}$)), indicating the presence of dynamical processes occurring in the micro- to millisecond range.

The two-field dispersion data obtained at 14.1 and 16.5 T for both linker and aromatic carbons were fitted according to the Luz–Meiboom equation[42] for a two-site fast exchange:

$$R_2 = R_2^0 + p_{major}(1 - p_{major})\Delta\omega^2 t_{exch}\left[1 - 4t_{exch}\nu_{CPMG}\tanh\frac{1}{4t_{exch}\nu_{CPMG}}\right] \quad (7)$$

where R_2^0 is the transverse relaxation rate in the absence of exchange, p_{major} is the relative population of the major state in exchange, $\Delta\omega$ corresponds to the resonance frequency difference between the spins in the major and minor states, and t_{exch} is the exchange time between the two states. Of course, the assumption of a two-site exchange is probably an oversimplification, but this model, which is usually the first employed for analyzing experimental data,[43] is adequate for having an estimation of the parameters of interest.

In order to get accurate parameters,[44] the two-field dispersion curves were fitted simultaneously for each case (linker and aromatic carbons) by using a nonlinear least-squares fitting procedure. The thermodynamic parameter p_{minor} (=1 − p_{major}), the structural parameter $\Delta\omega$, the kinetic parameter t_{exch}, and the relaxation rate in the absence of exchange R_2^0 deduced from the fitting of the ^{13}C transverse dispersion curves are listed in Table 8 for the two fields and the two temperatures investigated.

Considering the calculated errors, the results obtained for the linker and the aromatic carbons are quite similar as expected, showing the reliability of the method. In both cases, the population of the minor state is not affected by the temperature. The value found for p_{minor} is around 0.05, indicating the presence of a low-populated state. The exchange time t_{exch} is in the millisecond range, and the exchange rate, defined as ($1/t_{exch}$), is increasing with temperature, agreeing with the Arrhenius equation. Concerning the exchange-free relaxation rate R_2^0, it varies only little with the changes of temperature and field, with the transverse relaxation of the aromatic carbon being slightly faster. According to the $\Delta\omega$ values found for the linker and the aromatic carbons, the cryptophane-A minor state (if it would be visible on the spectrum) should appear a few thousand hertz away (roughly ±6–7 ppm at 298 K and ±8–10 ppm at 310 K) from the peaks corresponding to the major state. By comparing these results to those obtained by quantum chemical calculations (see Table 7), one can see that the $\Delta\omega$ values are consistent with the calculated chemical shifts when going from the *trans* conformers (which should correspond to the major state) to the *gauche* conformers (which could be attributed to the minor state).

Cross-Relaxation. The analysis of the ^{13}C relaxation dispersion curves revealed that a fast conformational exchange is occurring in the complexed cryptophane-A system. To complete this study and to give a possible solution of the above-mentioned conformational problem, it is relevant to measure the cross-relaxation rates between the linker protons and the aromatic proton number 3. After this, one can make comparisons with the distances from the DFT-optimized conformer structures: the cross-relaxation rates are proportional to the inverse sixth power of the corresponding proton–proton distance. The relevant distances are shown in Table 9.

One can see that a high cross-relaxation rate is expected in the case of the *gauche* conformers, since the distances are the shortest there. Very small values are expected for the $T_1T_1T_1$ conformer. The cross-relaxation data are shown in Tables 10 and 11.

It is interesting to notice that, in the case of dichloromethane complexes, there are no big differences between the two peaks in the spectrum. However, there is a big difference between the CH_2Cl_2 and $CHCl_3$ complexes in cryptophane-A. The cross-relaxation rate decreases by half in the case of the chloroform guest. This is not the case in cryptophane-But. This suggests that the conformational changes are much smaller in the case of the latter host. This is also indicated in the spectra: there are always

Table 8. Physicochemical Parameters Deduced from the Fitting of the ^{13}C Transverse Dispersion Curves[a]

		298 K		310 K	
		14.1 T	16.5 T	14.1 T	16.5 T
linker carbons (1′ and 2′)	p_{minor}	0.06 ± 0.01		0.04 ± 0.01	
	$\Delta\omega$ (Hz)	933 ± 71	1082 ± 83	1205 ± 130	1410 ± 152
	t_{exch} (ms)	1.1 ± 0.2		0.69 ± 0.05	
	R_2^0 (s^{-1})	5.3 ± 0.2	5.0 ± 0.2	4.8 ± 0.2	4.6 ± 0.2
aromatic carbon (6)	p_{minor}	0.07 ± 0.03		0.04 ± 0.01	
	$\Delta\omega$ (Hz)	1060 ± 175	1230 ± 203	1587 ± 175	1841 ± 203
	t_{exch} (ms)	1.0 ± 0.1		0.52 ± 0.04	
	R_2^0 (s^{-1})	6.1 ± 0.2	5.9 ± 0.3	5.6 ± 0.2	5.4 ± 0.3

[a]At 16.5 T, $\Delta\omega$ corresponds to (16.5/14.1) times the value obtained at 14.1 T. Errors are deduced from Monte Carlo iterations.

dx.doi.org/10.1021/jp4105272 | J. Phys. Chem. B 2014, 118, 2134–2146

Table 9. Distances between the Aromatic Proton 3 and the Linker Protons 1′ and 2′ in Å in DFT-Optimized Structures of Different Conformers of Cryptophane-A

$T_1T_1T_1$	3	$T_2T_2T_2$	3
1′	3.3	1′	3.6
1′	3.8	1′	2.8
2′	3.4	2′	3.6
2′	4.1	2′	2.8
$G_+G_+G_+$	3	G_G_G_	3
1′	2.4	1′	2.5
1′	2.4	1′	3.3
2′	4.2	2′	2.1
2′	4.5	2′	3.7

Table 10. Cross-Relaxation Rates (s^{-1}) between the Protons Attached to the Linker Carbons and the Aromatic Proton 3 for the Dichloromethane Complexes (Samples 4 and 7)

CH_2Cl_2@host		cryptophane-A		cryptophane-But	
T (K) (field)	^{1}H	^{1}H on C1	^{1}H on C2	^{1}H on C1	^{1}H on C2
235 (14.1 T)	3			1.01	0.82
240 (14.1 T)	3	0.54	0.43	0.69	0.56
255 (14.1 T)	3			0.25	0.28
258 (9.4 T)	3	0.15	0.13		

two peaks in the proton spectra of cryptophane-But, and the chemical shift difference between carbons 3 and 6 is also smaller. Looking at the cross-relaxation data at 258 K (the same temperature as used in cryptophane-C measurements[6]), it can be noted that the cross-relaxation rates in CH_2Cl_2@cryptophane-C are by a factor of 4 smaller. This indicates that even the CH_2Cl_2@cryptophane-A complex has *trans* character. The small cross-relaxation rate of $CHCl_3$ means that probably the $T_1T_1T_1$ conformer is preferred over the $T_2T_2T_2$. The high cross-relaxation rates of the $CHCl_3$ guest with both hosts (cryptophane-A, cryptophane-But) are very surprising and shed light on the possible problems with DFT calculations, namely, that the optimized structures are static and the systems are not. Consistently with the carbon-13 relaxation data, chloroform can be thought of as moving in a cone inside the cavity. The average distance of chloroform from the aromatic protons is 4 Å. It is impossible that one measures such a high cross-relaxation rate at this distance. In reality, this distance must be much shorter. This also means that the position of chloroform predicted by DFT is not fully correct. This can, in turn, perhaps be traced back to the lack of van der Waals contribution during the geometry optimization procedures.

CONCLUSIONS

The investigation of chloromethanes@cryptophane with the help of different NMR methodologies sheds light on the complexation process. Besides the fact that the chloromethane and the cryptophane diffuse as a single entity, it was also proven that a conformational variability/selection of encapsulation of chloromethane guests into the host cavity is also occurring. This phenomenon, already observed on variable temperature spectra, was studied further by DFT calculations and CPMG relaxation dispersion. These techniques gave structural information about the host but also allowed the determination of both kinetic and thermodynamic properties related to the conformational changes of the host. Nevertheless, the results obtained in this study for the solution state differ from the previously proposed induced fit model by Taratula et al. in the solid state.[40] Indeed, a double conformational selection model is proposed. Both the conformations of the methoxy groups and of the linkers play an important role in the case of cryptophane-A guest encapsulation, as in the case of cryptophane-C. This model was supported by the dynamical measurements of guest exchange and the activation energies. Moreover, the conformational changes of the host are different from those experienced in cryptophane-C. Here, the *trans* character plays an important role in the case of cryptophane-A, which can be caused by the methoxy groups being too close to each other when lying in the plane of the aromatic rings, which is their most stable position. In the case of cryptophane-But, the *gauche* character of the linkers is more pronounced and, as shown in the proton and carbon spectra, there is less change experienced by the host upon complex formation. Both hosts have a surprisingly high affinity constant to $CHCl_3$, compared to other cryptophane hosts. This can be explained by the volume differences of the conformers. In the case of cryptophane-C, the *gauche* conformers were more populated, while the *trans* conformers are more important in the case of cryptophane-A. For any of the hosts, the *trans* conformers have a bigger cavity. However, it should be noted that the explanation of the thermodynamic stability by the cavity size does not work in the case of cryptophane-But. It does explain the difference between dichloromethane complexes but not that between the chloroform encapsulation in various hosts. The stabilities of the chloroform complexes are very similar which is, at the present stage of the research, surprising and requires more investigation.

ASSOCIATED CONTENT

Supporting Information

Concentrations of the species in solution in the case of cryptophane-A complexes. Concentrations of the species in solution in the case of cryptophane-But complexes. ^{1}H spectrum of the solution containing 10 mM cryptophane-A and 60 mM

Table 11. Cross-Relaxation Rates (s^{-1}) between, on the One Hand, the Aromatic Protons and, on the Other, the Linker and Host Protons for the Chloroform Complexes (Samples 8, 9, and 10)

$CHCl_3$@host		cryptophane-A		cryptophane-But		
T (K) (field)	arom ^{1}H	^{1}H linker	C**H**Cl_3	^{1}H on C1	^{1}H on C2	C**H**Cl_3
240 K (14.1 T)	3	0.25	0.26	0.59	0.52	
	6	0.07	0.21	0.18	0.16	
258 K (9.4 T)	3	0.08	0.21	0.27	0.22	
	6	0.01	0.16			
260 K (16.5 T)	3					0.26
	6					0.24

dx.doi.org/10.1021/jp4105272 | J. Phys. Chem. B 2014, 118, 2134−2146

$CHCl_3$ in 1,1,2,2-CD_2Cl_4. Arrhenius plots of k_{-1} and k_1 exchange rate constants versus inverse temperature for dichloromethane and chloroform in cryptophane-A. Van't Hoff plots of the association constant K versus inverse temperature for dichloromethane and chloroform in cryptophane-A. Chemical shift difference of the aromatic ^{13}C signals and full width at half-height for cryptophane-A and both guests. Calculated chemical shifts for the linker and the aromatic carbons for the cryptophane-But host. Chemical shift difference of the aromatic ^{13}C signals and full width at half-height for cryptophane-But and both guests. Energies obtained by the geometry optimization of the conformers for the noncomplexed cryptophane-A. Energies obtained by the geometry optimization of the conformers for the $CHCl_3$ complexed cryptophane-A. This material is available free of charge via the Internet at http://pubs.acs.org.

AUTHOR INFORMATION

Corresponding Author

*E-mail: Jozef.Kowalewski@mmk.su.se.

Notes

The authors declare no competing financial interest.

ACKNOWLEDGMENTS

This work was supported by the Swedish Research Council (Grant No. 613-2011-3311). The generous grant from Knut and Alice Wallenberg Foundation, allowing the purchase of the 700 MHz NMR spectrometer for the Arrhenius Laboratory, is gratefully acknowledged. We thank Mr Torbjörn Astlind for his help with NMR spectrometers.

REFERENCES

(1) Gabard, J.; Collet, A. Synthesis of a (D_3)-Bis(cyclotriveratrylenyl) Macrocage by Stereospecific Replication of a (C_3)-Subunit. *J. Chem. Soc., Chem. Commun.* **1981**, 1137−1139.

(2) Collet, A.; Gabard, J.; Jacques, J.; Cesario, M.; Guilhem, J.; Pascard, C. Synthesis and Absolute Configuration of Chiral Structure of (M)-(−)-2,7,12-Triethoxy-3,8,13-Tris-[(*R*)-1-Methoxycarbonylethoxy]-10, 15-Dihydro-5H-Tribenzo[a,d,g]-Cyclononene. *J. Chem. Soc., Perkin Trans. 1* **1981**, 1630−1638.

(3) Cavagnat, D.; Brotin, T.; Bruneel, J. L.; Dutasta, J. P.; Thozet, A.; Perrin, M.; Guillaume, F. Raman Microspectrometry as a New Approach to the Investigation of Molecular Recognition in Solids: Chloroform-Cryptophane Complexes. *J. Phys. Chem. B* **2004**, *108*, 5572−5581.

(4) Nikkhou Aski, S.; Lo, A. Y. H.; Brotin, T.; Dutasta, J. P.; Edén, M.; Kowalewski, J. Studies of Inclusion Complexes of Dichloromethane in Cryptophanes by Exchange Kinetics and ^{13}C NMR in Solution and the Solid State. *J. Phys. Chem. C* **2008**, *112*, 13873−13881.

(5) Brotin, T.; Devic, T.; Lesage, A.; Emsley, L.; Collet, A. Synthesis of Deuterium-Labeled Cryptophane-A and Investigations of Xe@ Cryptophane Complexation Dynamics by 1D-EXSY NMR Experiments. *Chem.—Eur. J.* **2001**, *7*, 1561−1573.

(6) Takacs, Z.; Soltesova, M.; Kowalewski, J.; Lang, J.; Brotin, T.; Dutasta, J. P. Host-Guest Complexes between Cryptophane-C and Chloromethanes Revisited. *Magn. Reson. Chem.* **2013**, *51*, 19−31.

(7) Takacs, Z.; Brotin, T.; Dutasta, J. P.; Lang, J.; Todde, G.; Kowalewski, J. Inclusion of Chloromethane Guests Affects Conformation and Internal Dynamics of Cryptophane-D Host. *J. Phys. Chem. B* **2012**, *116*, 7898−7913.

(8) Cohen, Y.; Avram, L.; Frish, L. Diffusion NMR Spectroscopy in Supramolecular and Combinatorial Chemistry: An Old Parameter-New Insights. *Angew. Chem., Int. Ed.* **2005**, *44*, 520−554.

(9) Korzhnev, D. M.; Kay, L. E. Probing Invisible, Low-Populated States of Protein Molecules by Relaxation Dispersion NMR Spectroscopy: An Application to Protein Folding. *Acc. Chem. Res.* **2008**, *41*, 442−451.

(10) Kempf, J. G.; Loria, J. P. Measurement of Intermediate Exchange Phenomena. *Methods Mol. Biol.* **2004**, *278*, 185−231.

(11) Brotin, T.; Roy, V.; Dutasta, J. P. Improved Synthesis of Functional CTVs and Cryptophanes Using $Sc(OTf)_3$ as Catalyst. *J. Org. Chem.* **2005**, *70*, 6187−6195.

(12) Huber, G.; Beguin, L.; Desvaux, H.; Brotin, T.; Fogarty, H. A.; Dutasta, J. P.; Berthault, P. Cryptophane-Xenon Complexes in Organic Solvents Observed through NMR Spectroscopy. *J. Phys. Chem. A* **2008**, *112*, 11363−11372.

(13) Stott, K.; Keeler, J.; Van, Q. N.; Shaka, A. J. One-Dimensional NOE Experiments Using Pulsed Field Gradients. *J. Magn. Reson.* **1997**, *125*, 302−324.

(14) Emsley, L.; Bodenhausen, G. Gaussian Pulse Cascades: New Analytical Function for Rectangular Selective Inversion and In-Phase Excitation in NMR. *Chem. Phys. Lett.* **1990**, *165*, 469−476.

(15) Macura, S.; Farmer, B. T.; Brown, L. R. An Improved Method for the Determination of Cross-Relaxation Rates from NOE Data. *J. Magn. Reson.* **1986**, *70*, 493−499.

(16) Hu, H. T.; Krishnamurthy, K. Revisiting the Initial Rate Approximation in Kinetic NOE Measurements. *J. Magn. Reson.* **2006**, *182*, 173−177.

(17) Kowalewski, J.; Ericsson, A.; Vestin, R. Determination of NOE Factors Using the Dynamic Overhauser Enhancement Technique Combined with a Nonlinear Least-Squares-Fitting Procedure. *J. Magn. Reson.* **1978**, *31*, 165−169.

(18) Wagner, R.; Berger, S. Gradient-Selected NOESY-A Fourfold Reduction of the Measurement Time for the NOESY Experiment. *J. Magn. Reson., Ser. A* **1996**, *123*, 119−121.

(19) Bax, A.; Davis, D. G. Practical Aspects of Two-Dimensional Transverse NOE Spectroscopy. *J. Magn. Reson.* **1985**, *63*, 207−213.

(20) Griesinger, C.; Ernst, R. R. Frequency Offset Effects and Their Elimination in NMR Rotating-Frame Cross-Relaxation Spectroscopy. *J. Magn. Reson.* **1987**, *75*, 261−271.

(21) Wu, D. H.; Chen, A. D.; Johnson, C. S. An Improved Diffusion-Ordered Spectroscopy Experiment Incorporating Bipolar-Gradient Pulses. *J. Magn. Reson., Ser. A* **1995**, *115*, 260−264.

(22) Callaghan, P. T.; Le Gros, M. A.; Pinder, D. N. The measurement of Diffusion Using Deuterium Pulsed Field Gradient Nuclear Magnetic Resonance. *J. Chem. Phys.* **1983**, *79*, 6372−6381.

(23) Palmer, A. G., III; Skelton, N. J.; Chazin, W. J.; Wright, P. E.; Rance, M. Suppression of the Effects of Cross-Correlation between Dipolar and Anisotropic Chemical Shift Relaxation Mechanisms in the Measurement of Spin-Spin Relaxation Rates. *Mol. Phys.* **1992**, *75*, 699−711.

(24) Frisch, M. J.; Trucks, G. W.; Schlegel, H. B.; Scuseria, G. E.; Robb, M. A.; Cheeseman, J. R.; Scalmani, G.; Barone, V.; Mennucci, B.; Petersson, G. A.; et al. *Gaussian 09*, revision D.01; Gaussian, Inc.: Wallingford, CT, 2009.

(25) De Dios, A. C. Ab Initio Calculations of the NMR Chemical Shift. *Prog. NMR Spectrosc.* **1996**, *29*, 229−278.

(26) Barone, V.; Cossi, M. Quantum Calculation of Molecular Energies and Energy Gradients in Solution by a Conductor Solvent Model. *J. Phys. Chem. A* **1998**, *102*, 1995−2001.

(27) Cossi, M.; Rega, N.; Scalmani, G.; Barone, V. Energies, Structures, and Electronic Properties of Molecules in Solution with the C-PCM Solvatation Model. *J. Comput. Chem.* **2003**, *24*, 669−681.

(28) Grimme, S. Semiempirical GGA-Type Density Functional Constructed with a Long-Range Dispersion Correction. *J. Comput. Chem.* **2006**, *27*, 1787−1799.

(29) Binsch, G. In *Topics in Stereochemistry*; Eliel, E. L., Allinger, N. L., Eds.; John Wiley Sons, Inc.: Hoboken, NJ, 1968; Vol. 3, pp 97−191.

(30) Římal, V.; Štěpánková, H.; Štěpánek, J. Analysis of NMR Spectra in Case of Temperature Dependent Chemical Exchange Between Two Unequally Populated Sites. *Concepts Magn. Reson* **2011**, *38A*, 117−127.

(31) Garel, L.; Dutasta, J. P.; Collet, A. Complexation of Methane and Chlorofluorocarbons by Cryptophane-A in Organic Solution. *Angew. Chem., Int. Ed. Engl.* **1993**, *32*, 1169−1171.

(32) Lang, J.; Dechter, J. J.; Effemey, M.; Kowalewski, J. Dynamics of an Inclusion of Chloroform and Cryptophane-E: Evidence for a Strongly

Anisotropic van der Waals Bond. *J. Am. Chem. Soc.* **2001**, *123*, 7852−7858.
(33) Tosner, Z.; Lang, J.; Sandström, D.; Petrov, O.; Kowalewski, J. Dynamics of an Inclusion Complex of Dichloromethane and Cryptophane-E. *J. Phys. Chem. A* **2002**, *106*, 8870−8876.
(34) Lipari, G.; Szabo, A. Model-Free Approach to the Interpretation of Nuclear Magnetic Resonance Relaxation in Macromolecules. 1. Theory and Range of Validity. *J. Am. Chem. Soc.* **1982**, *104*, 4546−4559.
(35) Tosner, Z.; Petrov, O.; Dvinskikh, S. V.; Kowalewski, J.; Sandström, D. A ^{13}C Solid-State NMR Study of Cryptophane-E: Chloromethane Inclusion Complexes. *Chem. Phys. Lett.* **2004**, *388*, 208−211.
(36) Petrov, O.; Tosner, Z.; Csöregh, I.; Kowalewski, J.; Sandström, D. Dynamics of Chloromethanes in Cryptophane-E Inclusion Complexes: A ^{2}H Solid-State NMR and X-Ray Diffraction Study. *J. Phys. Chem. A* **2005**, *109*, 4442−4451.
(37) Frish, L.; Matthews, S. E.; Böhmer, V.; Cohen, Y. A Pulsed Gradient Spin Echo NMR Study of Guest Encapsulation by Hydrogen-Bonded Tetraurea Calix[4]arene Dimers. *J. Chem. Soc., Perkin Trans. 2* **1999**, 669−671.
(38) Hof, F.; Craig, S. L.; Nuckolls, C.; Rebek, J., Jr. Molecular Encapsulation. *Angew. Chem., Int. Ed.* **2002**, *41*, 1488−1508.
(39) Brotin, T.; Dutasta, J. P. Cryptophanes and Their Complexes − Present and Future. *Chem. Rev.* **2009**, *109*, 88−130.
(40) Taratula, O.; Hill, P. A.; Khan, N. S.; Carroll, P. J.; Dmochowski, I. J. Crystallographic Observation of "Induced Fit" in a Cryptophane Host-Guest Model System. *Nat. Commun.* **2010**, *1*, 148.
(41) Brotin, T.; Cavagnat, D.; Dutasta, J. P.; Buffeteau, T. Vibrational Circular Dichroism Study of Optically Pure Cryptophane-A. *J. Am. Chem. Soc.* **2006**, *128*, 5533−5540.
(42) Luz, Z.; Meiboom, S. Nuclear Magnetic Resonance Study of the Protolysis of Trimethylammonium Ion in Aqueous Solution-Order of the Reaction with Respect to Solvent. *J. Chem. Phys.* **1963**, *39*, 366−370.
(43) Kleckner, I. R.; Foster, M. P. An Introduction to NMR-Based Approaches for Measuring Protein Dynamics. *Biochim. Biophys. Acta* **2011**, *1814*, 942−968.
(44) Kovrigin, E. L.; Kempf, J. G.; Grey, M. J.; Loria, J. P. Faithful Estimation of Dynamics Parameters from CPMG Relaxation Dispersion Measurements. *J. Magn. Reson.* **2006**, *180*, 93−104.